Research Paper

Characterization of spontaneously generated prion-like conformers in cultured cells

Roger S. Zou[1], Hisashi Fujioka[2, 5, 6], Jian-Ping Guo[8], Xiangzhu Xiao[1], Miyuki Shimoji[1], Crystal Kong[1], Cecilia Chen[1], Megan Tasnadi[1], Chesinta Voma[1], Jue Yuan[1], Mohammed Moudjou[9], Hubert Laude[9], Robert B. Petersen[1, 3, 4], Wen-Quan Zou[1, 3, 7 *]

[1] Departments of Pathology, [2]Pharmacology, [3]Neurology, and [4]Neuroscience, [5]Electron Microscopy Facility, [6]Center for Mitochondrial Disease, [7]National Prion Disease Pathology Surveillance Center, Case Western Reserve University School of Medicine, 2085 Adelbert Road, Cleveland, Ohio 44106, USA
[8]Kinsmen Laboratory of Neurological Research, University of British Columbia, Vancouver, BC V6T 1Z3, Canada
[9]Virologie Immunologie Moléculaires, UR892 INRA 78350 Jouy-en-Josas, France

Running title: *Insoluble PrP and mutation*
Keywords: *Prion protein, prion disease, insoluble prion protein, neuroblastoma cells, mutation, autophagy*

Received: 9/24/11; Accepted: 10/03/11; Published: 10/09/11
Correspondence to Wen-Quan Zou, wenquan.zou@case.edu

Abstract: A distinct conformational transition from the α-helix-rich cellular prion protein (PrP^{C}) into its β-sheet-rich pathological isoform (PrP^{Sc}) is the hallmark of prion diseases, a group of fatal transmissible encephalopathies that includes spontaneous and acquired forms. Recently, a PrP^{Sc}-like intermediate form characterized by the formation of insoluble aggregates and protease-resistant PrP species termed insoluble PrP^{C} ($iPrP^{C}$) has been identified in uninfected mammalian brains and cultured neuronal cells, providing new insights into the molecular mechanism(s) of these diseases. Here, we explore the molecular characteristics of the spontaneously formed $iPrP^{C}$ in cultured neuroblastoma cells expressing wild-type or mutant human PrP linked to two familial prion diseases. We observed that although PrP mutation at either residue 183 from Thr to Ala (PrP^{T183A}) or at residue 198 from Phe to Ser (PrP^{F198S}) affects glycosylation at both N-linked glycosylation sites, the T183A mutation that results in intracellular retention significantly increased the formation of $iPrP^{C}$. Moreover, while autophagy is increased in F198S cells, it was significantly decreased in T183A cells. Our results indicate that $iPrP^{C}$ may be formed more readily in an intracellular compartment and that a significant increase in PrP^{T183A} aggregation may be attributable to the inhibition of autophagy.

INTRODUCTION

The abnormal proteinase K (PK)-resistant prion protein (PrP^{Sc}) is the only known component of the infectious prions that are associated with a group of fatal neurodegenerative disorders called prion diseases or transmissible spongiform encephalopathies [1]. While it has been well documented that PrP^{Sc} is derived from a PK-sensitive cellular PrP^{C} in the central nervous system through an alpha-helix to beta-sheet structural transition, the specific molecular mechanism(s) behind the PrP conversion remain poorly understood [2]. Several plausible theories have emerged, including the prevailing seeding model [3], which explains this conversion with the use of PrP^{Sc} seeds that are introduced either by exogenous infection in diseases such as kuru, iatrogenic Creutzfeldt-Jakob disease (CJD) and variant CJD, or formed by endogenous PrP^{Sc} molecules including sporadic CJD and various familial prion diseases. However, the exact molecular nature of the endogenous PrP^{Sc} has not been elucidated.

In 2006, we first identified small amounts of PK-resistant PrP aggregates in uninfected brains of humans, cattle and hamsters [4]. Since then, subsequent studies have revealed similar insoluble structures in a wide

range of organisms, from cattle and sheep to humans [5] and cultured neuroblastoma cells expressing wild-type or mutant human PrP [6]. All these studies provide experimental evidence that prion-like forms are present at a low level in the normal brain. Such isoforms could be either the silent prions or prion precursors proposed previously [3,7] or the recognized PrP species implicated in long-term memory in healthy humans [8]. Neuroblastoma cell expressing various human PrP mutants are an essential tool in the study of mutant prions linked to naturally occurring familial prion diseases [9-11,6]. Previously, using two models expressing either the mutations at residue 183 from Thr to Ala (PrP^{T183A}) or at residue 198 from Phe to Ser (PrP^{F198S}), we discovered a PK-resistant PrP (PrP^{res}) species that exhibited higher affinity for anti-PrP monoclonal antibody 1E4, with an epitope between residues 97 and 105 [6], compared to anti-PrP antibody 3F4, an antibody widely-used in the detection of human prions with an epitope between residues 106 and 112 [12]. Furthermore, we demonstrated that the immunoreactivity behavior and gel mobility of this PrP^{res} is virtually identical to those of PrP^{*20} that we observed previously in uninfected brain [4,6], validating the cell model for the investigation of the spontaneously formed $iPrP^{C}$.

In this study, using cells expressing PrP^{Wt}, PrP^{T183A} and PrP^{F198S}, we made the following observations. First, these PrP mutations increased aggregation of the protein, of which PrP^{T183A} that has been reported to accumulate intracellularly [10] exhibited the highest amount of iPrP. Second, immunofluorescence microscopy demonstrated that 1E4 had lower affinity for PrP in cultured cells than 3F4, as on immunoblots. Third, glycans at the second site (N197) are basic, whereas glycans at the first site (N181) are acidic. Fourth, the T183A mutation not only abolished glycosylation at N181, but also altered glycosylation at N197. In addition to the immaturity of the glycan at N197 reported previously [10], the composition of N197 may be also changed, as evidenced by the faster migration of N197 on PK-resistant PrP^{T183A} compared to that of N181 on the PK-resistant PrP^{F198S} or PrP^{Sc} from sCJD. Fifth, the F198S mutation also altered glycosylation at both the first and second sites. The glycosylation on the diglycosylated PrP^{F198S} seemed to be more mature than that on the monoglycosylated protein. Using monoclonal antibodies V14 and V61 that differentiate the two monoglycosylated PrP (Moudjou et al., 2004), we observed that the mutation blocked the V14 epitope, which was mimicked by reduction and alkylation, a reaction that often breaks disulfide bond and prevents re-oxidation of the thiol group [13]. Although V61 detected unglycosylated PrP and PrP monoglycosylated at N197 (mono197) in the brain PrP, it failed to detect the glycosylated and de- or un-glycosylated PrP from cultured neuronal cells. Finally, electron microscopy revealed that while cells expressing PrP^{F198S} enhanced autophagy, PrP^{T183A} seemed to completely inhibit autophagy compared to wild-type cells. Our findings provide new insights into the molecular mechanisms underlying the formation of $iPrP^{C}$ and abnormal folding of mutant proteins.

RESULTS

Prediction of the effects of mutations on molecular weights, charges, and glycosylation of human PrP. We first predicated the effects of PrP^{T183A} and PrP^{F198S} on molecular weights and charges of the protein using the ProtParam tool at the website of http://web.expasy.org/protparam/ from the ExPASy; the molecular weight of the wild type prion protein (PrP^{Wt}) backbone from residues 23 to 231 is 22,834.1 Dalton (Da). Compared to PrP^{Wt}, the molecular weights of PrP^{T183A} and PrP^{F198S} were decreased (22,834.1 Da vs. 22,804.1 Da; 22,834.1 Da vs. 22,774.0 Da). Although the molecular weight of PrP^{F198S} decreased more than that of PrP^{T183A} compared to wild type controls, the small degree of change in the molecular weight might not be detectable by Western blotting. In addition, all three PrP molecules exhibited the same molecular charge with a theoretical isoelectric point (*p*I) of 9.39.

The N-linked glycosylation prediction algorithm NetNGlyc 1.0 was then used at http://www.cbs.dtu.dk/services/NetNGlyc to predict the likelihood of glycosylation at the two consensus sites. The NetNGlyc server provides a glycosylation potential value between 0 and 1 for each N-linked glycosylation site. A potential value greater than 0.5 indicates that glycosylation is probable at the site. Using this algorithm, the glycosylation potential values of N181 and N197 in PrP^{Wt} were determined to be 0.6636 and 0.7197, respectively. Notably, the potential value was greater at the second site than at the first site in all three species tested (PrP^{Wt}, PrP^{T183A} and PrP^{F198S}). Glycosylation at only N197, but not N181, was predicted in the PrP^{T183A} mutation (0.7196, almost identical to that of PrP^{Wt}), while the first and second glycosylation sites were predicted for PrP^{F198S} (0.6633 and 0.6988, respectively). Interestingly though, the potential value at the second site was decreased for

PrP^{F198S} compared to that in PrP^{Wt} (0.6988 vs. 0.7197), suggesting that the F198S mutation mainly affects glycosylation at N197. The expectation would be that the mutation from Phe to Ser at 198 would increase glycosylation [14].

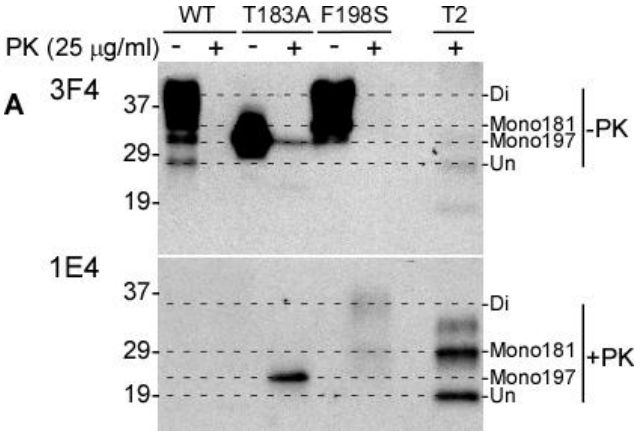

Figure 1. Detection of untreated and PK-treated PrP from three types of cultured cells with 3F4 and 1E4. ***A:*** Western blotting of cell lysates with or without PK-treatment at 25 μg/ml) probed with 3F4 (upper panel) and 1E4 (lower panel). WT: Lysates of cells expressing PrP^{Wt}. T183A: Lysates of cells expressing PrP^{T183A} mutation. F198S: Lysates of cells expressing PrP^{F198S}. T2: PrP^{Sc} type 2 control from sCJD. Di: Diglycosylated PrP. Mono181: PrP monoglycosylated at the first site. Mono197: PrP monoglycosylated at the second site. Un: Unglycosylated PrP. Comparison of affinities of 1E4 and 3F4 antibodies to the full-length and N-terminally truncated human PrP. The dashed-lines are used to align PrP bands on the blots.

PK-resistant PrP conformers detected preferentially by the 1E4 anti-PrP antibody in cultured neuronal cells. As reported previously [10,11,6], PrP^{T183A} and PrP^{F198S} have altered gel profiles, largely because of the effect of the mutations on glycosylation. Probed with the 3F4 antibody directed against PrP106-110 [12], PrP^{Wt} migrated as three major bands of one di-glycosylated (~36-48 kDa), two mono-glycosylated (~34-36 kDa and ~32-33 kDa, respectively), and one un-glycosylated (27-28 kDa) forms (Fig. 1A, upper panel). In contrast, a single band migrating at 28-36 kDa, corresponding to the monoglycosylated PrP, was detectable in cell lysates from PrP^{T183A} expressing cells (Fig. 1A, upper panel). Bands migrating at 37-45 kDa and 33-36 kDa corresponding to the di- and mono-glycosylated forms, respectively, were detected in cell lysates from PrP^{F198S} expressing cells; the unglycosylated form was undetectable. From these data, we can conclude that PrP^{T183A} mainly contains monoglycosylated PrP at the second site (mono197), whereas PrP^{F198S} contains one di- and two separate mono-glycosylated PrP occupied at the first (mono181) or mono197. After treatment with PK at 25 μg/ml, no PrP was detected except from PrP^{T183A} expressing cells, in which a weak band with no change in migration remained when probed with 3F4. This band was un-digested PrP^{T183A}.

In contrast, using the anti-PrP monoclonal antibody 1E4 directed against PrP97-105 [6], untreated PrP was virtually undetectable in all three cell lysates before PK treatment while 1E4 detected mutant, but not wild type, PK-resistant forms (Fig. 1A). One theory for this unique behavior of the 1E4 antibody is that the 1E4 epitope is blocked in full-length PrP, even when subjected to denaturing conditions prior to Western blotting, and becomes exposed only when truncated by PK with the removal of approximately 60-70 amino acids from the N-terminus [6].

In the cell lysates probed with 1E4, the profile of PK-resistant PrP^{F198S} was different from that of PrP^{T183A}. In the T183A samples, 1E4 revealed an intense band migrating at 23-25 kDa corresponding to the PK-resistant monoglycosylated species (Fig. 1A, lower panel). PrP^{F198S} had two PK-resistant bands: a ~32-39 kDa band corresponding to di-glycosylated PrP and a ~26-29 kDa band corresponding to monoglycosylated PrP (Fig. 1A, lower panel). Interestingly, the mobility of di- but not mono-glycosylated PrP^{F198S} was slightly slower than that of PK-resistant PrP^{Sc} from sCJD (Fig. 1A, lower panel) while the mobility of the monoglycosylated PrP^{T183A} (second site) was faster not only than that of the monoglycosylated form of PrP^{F198S} from cell lysates, but also than that of PrP^{res} from the CJD brain control. Because the monoglycosylated PrP^{T183A} carries glycans at the second glycosylation site at residue 197, the monoglycosylated form of PrP^{res} from CJD brains and of PrP^{F198S} from cultured cells with slower migration may represent glycans at the first glycosylation site, residue 181. Another possibility is that the glycans at the N197 site are modified differently and consequently migrate slower than glycans from PrP^{T183A}.

Utilizing immunofluorescence tagging and microscopy, we next compared cells expressing PrP^{Wt}, PrP^{T183A} and PrP^{F198S} by immunostaining with 1E4 or 3F4. Consistent with Western blotting, all three cell types exhibited greater immunostaining with 3F4 than with 1E4 (Fig. 1B). Notably, although weak, PrP^{Wt} and two PrP mutants became detectable by immunofluorescence with 1E4, in contrast to results by Western blotting with

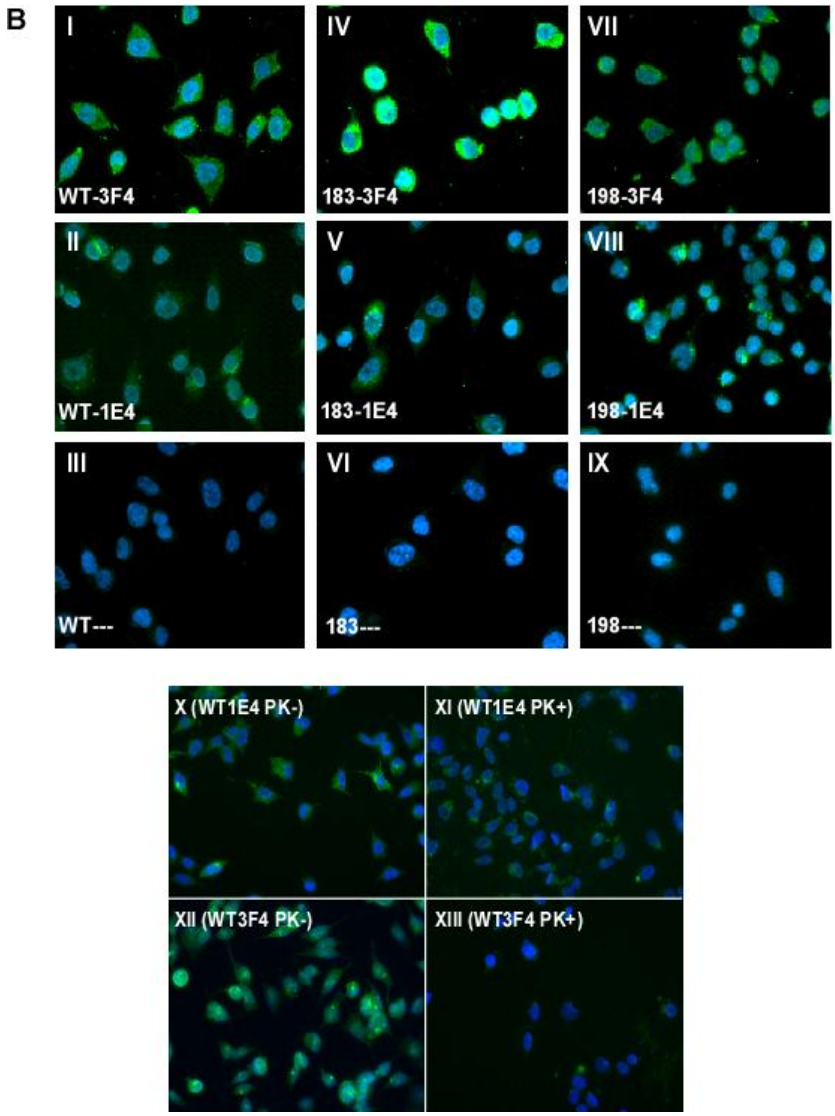

Figure 1. Detection of untreated and PK-treated PrP from three types of cultured cells with 3F4 and 1E4. ***B:*** Immunofluorescence detection of untreated and treated PrP with 3F4 and 1E4. Panels I-III: Cells expressing human PrP^{Wt}. Panels IV-VI: Cells expressing human PrP^{T183A}. Panels VII-IX: Cells expressing human PrP^{F198S}. Panels I, IV, and VII: Staining with 3F4. Panels II, V, and VIII: Staining with 1E4. Panels III, VI, and IX: Staining without anti-PrP antibodies. Panels X and XI: Wild-type cells staining with 1E4 before and after PK-treatment. Panels XII and XIII: Wild-type cells staining with 3F4 before and after PK-treatment.

1E4 shown in Fig. 1A. In addition, as demonstrated previously, PrP^{T183A} is most likely located intracellularly, while wild type and PrP^{F198S} are present on the cell surface [10]. 3F4 immunostaining was reduced to almost insignificant levels when wild type cells were treated with PK (Fig. 1B), consistent with Western blotting results. In contrast, 1E4 immunostaining was decreased after PK-treatment, which was opposite to that observed in Western blots.

Comparison of PrP oligomeric state between wild-type and mutant PrP. Sucrose step gradient sedimentation is a technique used to separate prion protein species based on their density, size, and conformation [15,4]. In general, monomers or small oligomers are often recovered in the top fractions, whereas large aggregates are recovered in the bottom fractions after ultracentrifugation on the sucrose step gradients. An increase in the formation of PK-resistant PrP species in cells expressing mutant PrP might be associated with an increase in the aggregation of the protein. The distribution of PrP in 11 sucrose step gradients fractions collected after ultracentrifugation was determined by Western blotting probed with the 3F4 antibody. As expected, most PrP^{Wt} was recovered in the top fractions, i.e. fractions 1-2, whereas a small

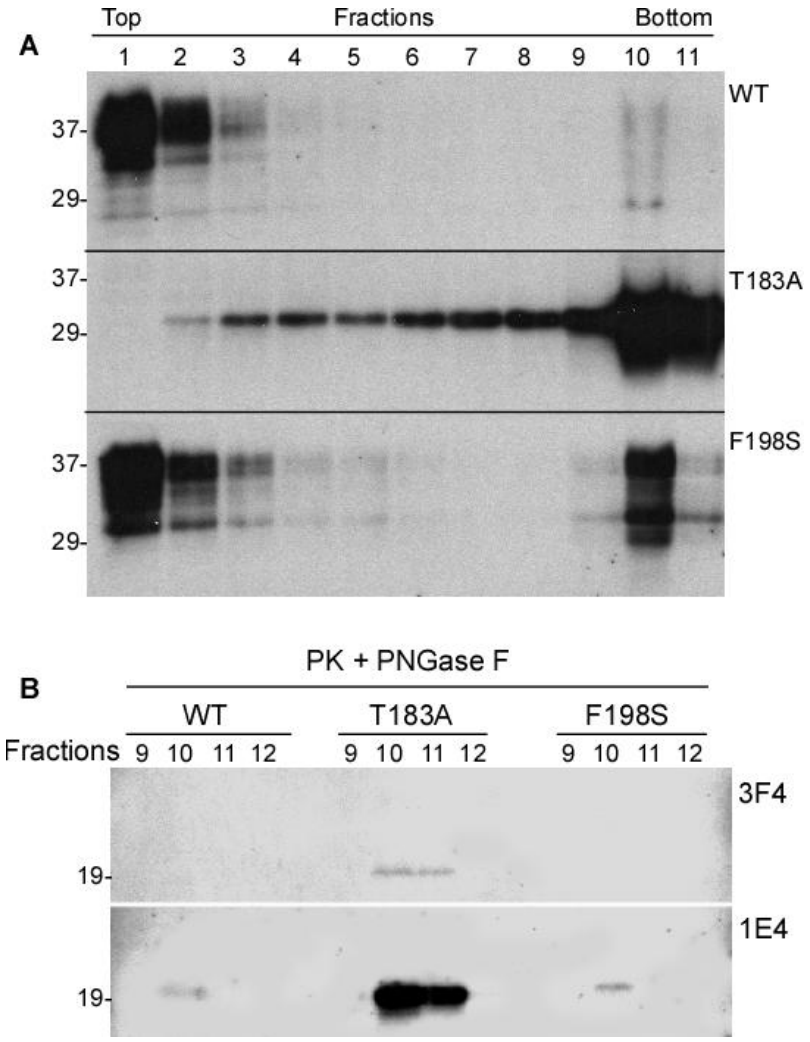

Figure 2. Detection of oligomeric state of wild-type and mutant PrP. PrP from three types of cells were subjected to sucrose step gradient sedimentation. ***A:*** PrP in the fractions of the gradients was detected by Western blotting with 3F4. Upper panel: PrP^{Wt}. Middle panel: PrP^{T183A}. Lower panel: PrP^{F198S}. ***B:*** PrP in fractions 9-12 was treated with PK and PNGase F prior to Western blotting with 3F4 (upper panel) and 1E4 (lower panel).

amount of PrP was observed in fraction 10. In contrast, significant amounts of PrP^{T183A} were recovered in the bottom fractions, whereas no PrP^{T183A} was detected in fraction 1. Only a very small amount of PrP was observed in fraction 2 (Fig. 2A, middle panel). Compared to PrP^{Wt}, although most of PrP^{F198S} was distributed in the top fractions 1-2, an increased amount of PrP^{F198S} was also recovered in bottom fractions, especially in fraction 10 (Fig. 2A, lower panel).

To determine which fractions contain PK-resistant wild-type or mutant PrP, we treated PrP from fractions 1 to 11 with PK and PNGase F (Fig. 2B). PK-resistant PrP^{T183A} was only detected in fractions 10 and 11 when probed with 3F4; other fractions did not show any PK-resistance. In addition, 3F4 did not detect PK resistant wild type and F198S mutant PrP in any sucrose gradient fraction, while 1E4 detected PK-resistant iPrP in all three PrP species, with the highest intensity in the T183A mutant PrP (Fig. 2B). However, small amounts of PK-resistant PrP were only observed in fraction 10 for PrP^{Wt} and PrP^{F198S}, whereas a larger amount of PK-resistant PrP was detected in fractions 10 and 11 for PrP^{T183A}.

Two-dimensional gel electrophoresis of $iPrP^{C}$ from cultured neuronal cells expressing PrP^{Wt}, PrP^{T183A}, or PrP^{F198S}. The above one-dimensional (1-D) electrophoresis and immunoblotting clearly indicated that glycans at the two N-linked glycosylation sites of the PK-resistant $iPrP^{C}$ are different in their molecular weight: the monoglycosylated PrP species at the second site, residue 197 (mono197), migrated faster than those monoglycosylated at the first site, residue 181

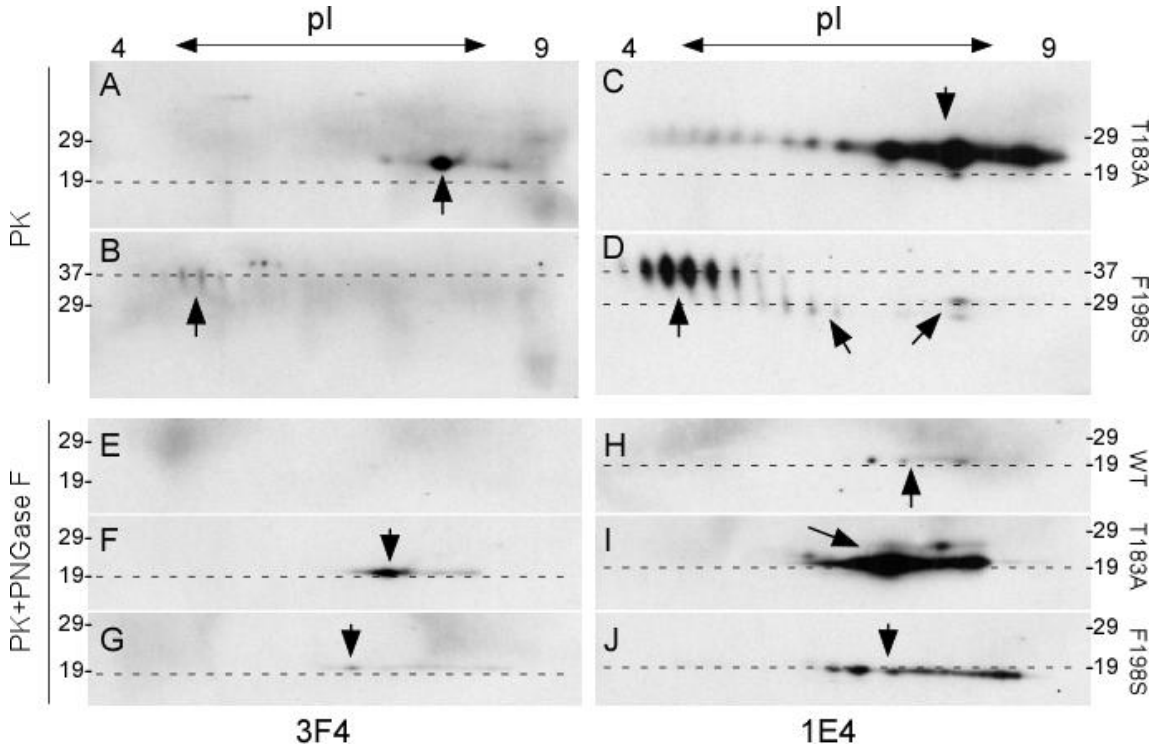

Figure 3. Two-dimensional gel electrophoresis and blotting of wild-type and mutant PrP captured by g5p and treated with PK or with PK plus PNGase F. ***A-D:*** Cell lysates containing PrP^{T183A} (***A*** and ***C***) or PrP^{F198S} (***B*** and ***D***) were treated with PK at 25 μg/ml prior to Western blotting. ***E-J***: Cell lysates containing PrP^{Wt} (***E*** and ***H***), PrP^{T183A} (***F*** and ***I***), or PrP^{F198S} (***G*** and ***J***) were treated with PK plus PNGase F prior to Western blotting. PrP spots are highlighted by arrows. The dashed-lines are aligned with molecular weight makers. Blots ***A***, ***B***, ***E***, ***F***, and ***G*** were probed with 3F4, whereas blots ***C***, ***D***, ***H***, ***I***, and ***J*** were probed with 1E4.

(mono181). Taking advantage of the unique PrP^{T183A} mutation that eliminates the first but retains the second glycosylation site, we next asked whether mono197 and mono181 have distinct molecular charges by two-dimensional (2-D) gel electrophoresis, a technique that separates proteins based on both molecular weight and molecular charge. The gene 5 protein (g5p) was first used to isolate $iPrP^{C}$ from the three types of cell lysates, following a previously described protocol [4,6].

Similar to 1-D immunoblotting, no convincing PK-resistant PrP^{Wt} spots were detected by 3F4 or 1E4 on 2-D blots (data not shown). However, the two PK-resistant mutants were detected by both 1E4 and 3F4, although the PrP intensity of the former was 5-10 fold greater using 1E4 compared to 3F4. The T183A mutant blots probed with 3F4 showed PK-resistant prion protein migrating at 23-26 kDa with isoelectric points (*p*I) from pH 8.0 to 9.5. An intense spot at pH 8.8 was also detected (Fig. 3A, arrow). These spots are believed to correspond to mono197 since the first glycosylation site is eliminated by the T183A mutation. The F198S mutant protein migrated at ~36-38 kDa with *p*I from pH 4.5 to 5.5. Based on their molecular weights, these spots represent di-glycosylated PrP species (Fig. 3B). However, spots detected using the 1E4 antibody were more intense and had noticeable differences on both blots. PrP^{T183A} spots detected by 1E4 migrating at ~22-27 kDa corresponding to mono197 were mainly detected in a range from pH 7.5 to 10.0 with faint spots also detectable at pH 4 (Fig. 3C). PrP^{F198S} spots were mainly detected between pH 4.5 and 6 migrating at ~35-39 kDa, corresponding to di-glycosylated forms (Fig. 3D). Two populations of faint PrP spots migrating at ~27-30 kDa were also detected between pH 6.2 and 7.2 as well as between pH 8.0 and 9.5, corresponding to mono181 or mono197. Spots migrating at ~27-30 could be PrP species monoglycosylated at the first site since they shared the similar molecular weight with mono181 identified by 1-D blotting (Fig. 1 and 3D), whereas spots between pH 8.0 and 9.5 migrating at ~24-26 kDa could be the monoglycosylated at the second site (Fig. 3D).

After treatment with PK and PNGase F, the two mutants exhibited PK-resistant forms, but not the wild type (Fig.

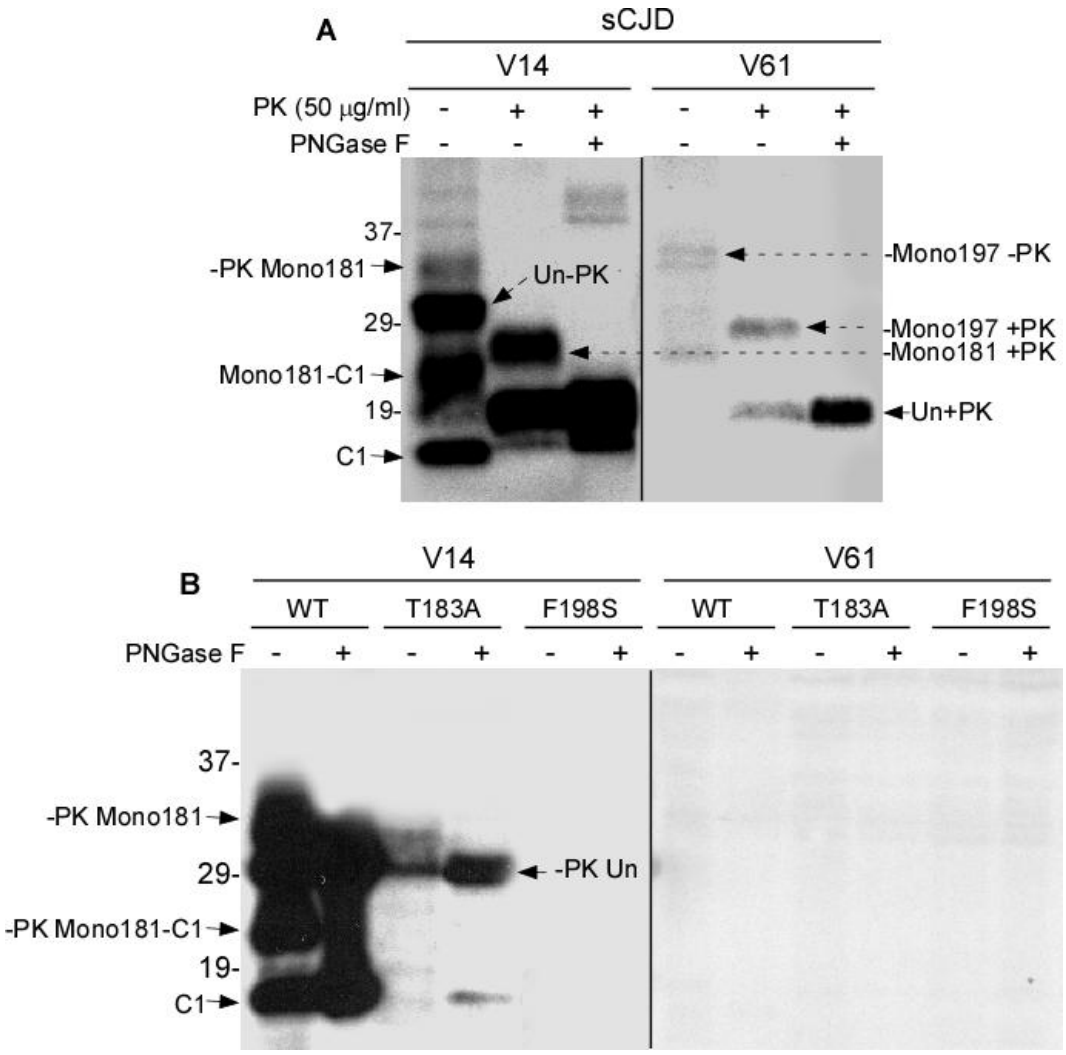

Figure 4. Western blotting of PrP with V14 and V61. ***A:*** PrP^{Sc} from sCJD untreated or treated with PK or PK plus PNGase F was probed with V14 or V61. ***B:*** PrP^{Wt}, PrP^{T183A} or PrP^{F198S} from cells untreated or treated with PNGase F was probed with V14 or V61.

3E-G). The PK-resistant PrP^{T183A} and PrP^{F198S} forms detected with 3F4 exhibited similar gel mobility at 19-20 kDa with pH between 7.0 and 9.5 on the blots, although there was a slight difference in pH between the most intense spots (Fig. 3F and 3G). However, in samples probed with the 1E4 antibody, the PK-resistant $iPrP^{C}$ became detectable even for PrP^{Wt}. The faint wild type spots migrating at ~19-20 kDa with pH 7.5-8.5 (Fig. 3H) while more intense PK-resistant PrP^{T183A} and PrP^{F198S} spots were detected with similar gel mobility migrating at ~19-20 kDa and pH 7-9.5 (Fig. 3I and 3J). Furthermore, these 2-D analyses of glycosylated and deglycosylated PK-resistant mutant iPrP indicated that glycans at the second site are more basic, whereas glycans at the first site are more acidic. 2-D blots, similar to the 1-D immunoblotting, also demonstrated that 1E4 has higher affinity for PK-resistant iPrP compared to 3F4. As indicated above, the effect of the two mutations by themselves on the charge of the proteins was not predicted. Two possibilities that may explain the slight differences in the pH of intense spots after deglycosylation: the three types of proteins have either distinct N-terminal protease cleavage sites or distinct GPI anchors.

Detection of PrP^{Wt}, PrP^{T183A}, or PrP^{F198S} with anti-PrP antibodies directed against different N-linked glycosylation sites. Previous studies indicated that PK-resistant monoglycosylated PrP^{T183A} has a molecular weight lower than the PK-resistant monoglycosylated PrP^{F198S} or PrP^{Sc}. This observation may be due to two possibilities: First, there may be abnormal glycosylation at N197 on PrP^{T183A}, even though this mutation directly eliminates N181. Second, the molecular weight the

glycans is greater in mono181 than in mono197. However, this hypothesis is inconsistent with a previous report [16]. In the previous study, two monoclonal antibodies termed V14 and V61 were generated using recombinant sheep PrP as an immunogen to produce glycan-controlled epitopes on the PrP molecule, which discriminate between the two monoglycosylated species [16,17]. Notably, the epitopes recognized by the two antibodies were identified in 2.5-Å-resolution crystal structures of the PrP-antibody complex; the epitopes could not be mapped using conventional peptide scanning [16,18, 17]. It was observed that the V14 epitope is localized between sheep PrP188 and 199 corresponding to human PrP185-196, whereas the V61 epitope has not been determined precisely yet. The V61 epitope was deduced to locate in the region before amino acid 171 to the first glycosylation site [16,17]. Interestingly, although both antibodies recognize unglycosylated PrP, V14 binds to PrP with the first Asn glycosylation site occupied (corresponding to human mono181) and V61 binds to PrP carrying the second glycosylation site (corresponding to human mono197) from sheep, humans, hamsters, and mice. It was also reported that the glycan chain was smaller at the first glycosylation site than at the second site [16].

We first examined PrP^{Sc} that was untreated, treated with PK alone, or treated with PK plus PNGase F from sCJD brains with the two antibodies. Without PK or PNGase F treatment, five major PrP bands were detected by V14 (Fig. 4A). Based on the molecular weight, the top band migrating at ~33-35 kDa represents the monoglycosylated PrP species. Since V14 detects PrP species monoglycosylated at N181, this band is mono181. The second band migrating at ~29-32 kDa corresponds to the unglycosylated full-length PrP. The third band migrating at ~ 23-25 is the monoglycosylated C1 fragment with the first site occupied (mono181- C1). The fourth band migrating at 19-20 kDa is the unglycosylated C2 fragment, an endogenously N-terminally truncated PrP fragment detected in CJD brains [19]. Finally, the fifth band migrating at ~18 kDa is unglycosylated C1 that is N-terminally truncated in normal brains [19]. After PK-treatment, only three major bands are detectable with V14. The top band migrating at ~26-28 is PK-resistant PrP monoglycosylated at the first site (mono181 +PK). The second band migrating at ~19 kDa is PK-resistant unglycosylated PrP (Un + PK). The third faint band was detected at ~18.5 kDa. In the samples treated with both PK and PNGase F, only two bands were detectable: the dominant band migrated at ~19-20 kDa, while the other migrated at ~18.5 kDa. Compared to the samples treated with PK, but without PNGase F, the band migrating at ~18.5 kDa significantly increased, suggesting that this new fragment contains both glycosylated and unglycosylated forms. Moreover, since it was not detected in the untreated samples, this new fragment could be generated by PK digestion *in vitro* (Fig. 4A, left panel).

Although equal amounts of samples were used, in general, the PrP intensity was much lower in samples probed with V61 than in samples probed with V14 (Fig. 4A, right panel). The intensity of PrP bands in the untreated PrP detected with V61 was weak and four bands could be identified. The top double bands migrating at 34-36 kDa corresponds to the PrP species monoglycosylated at the second glycosylation site (mono197 -PK). The band migrating at ~29-31 kDa corresponds to the unglycosylated full-length PrP. The band migrating at ~27-28 kDa represents C1 monoglycosylated at the second site (mono197-C1). After treatment with PK, two bands became detectable migrating at ~29-30 kDa and 19-20 kDa, respectively. Since V61 detected the monoglycosylated species occupied at residue 197, they represent the PK-resistant PrP species monoglycosylated at the second site (mono197 +PK) and PK-resistant deglycosylated and unglycosylated forms (Un +PK). Consistent with the observation by Moudjou et al., the migration of the PrP mono197 detected with V61 was slower than that of PrP mono181 detected with V14 (Fig. 4A). Therefore, using the two antibodies, we observed that the human PK-resistant PrP species monoglycosylated at the second site (mono197) has a higher molecular weight than that monoglycosylated at the first site (mono181). In addition, both antibodies were unable to detect di-glycosylated human PrP, consistent with the previous observation by Moudjou et al. [16].

In cultured neuronal cell lysates containing PrP^{Wt}, four major bands were detected by V14, migrating at ~33-35 kDa, ~29-32 kDa, ~23-25 kDa, and ~18 kDa (Fig. 4B, left panel). They correspond to mono181, unglycosylated PrP, mono181-C1, and unglycosylated C1. Compared to PrP^{Sc} from sCJD in Fig. 4A, C2 was dramatically decreased in uninfected cell lysates. After treatment with PNGase F, only two bands were detected, corresponding to deglycosylated full-length at ~29-32 kDa and N-terminally truncated C1 at 18 kDa. V14 mainly detected the unglycosylated PrP^{T183A} migrating at ~29-32 kDa. Faint bands were also detected migrating at ~19 kDa and 18 kDa

corresponding to C2 and C1, respectively (Fig. 4B, left panel). After deglycosylation with PNGase F, two bands corresponding to deglycosylated and unglycosylated full-length and N-terminally truncated PrP molecules were detected by V14. In contrast, no bands were detected by V14 in treated and untreated cell lysates containing PrP^{F198S}. Surprisingly, no PrP bands were detected by V61 in all three cell lysates untreated and treated with PNGase F (Fig. 4B, right panel). Using the two antibodies we were unable to address issues why the migration of the mono197 from PrP^{T183A} is faster than that of PrP^{F198S} because of inability of V14 to detect PrP^{F198S} and because of inability of V61 to detect both wild-type and mutant PrP from cultured cell lysates. Nevertheless, our current study revealed that V14 identified a C1 monoglycosylated at the second glycosylation site (mono197-C1). Moreover, our new results for the first time indicated that F198S mutation blocked the binding of V14 to PrP and the V61 epitope was completely blocked in both wild-type and mutant PrP from cultured cells.

Effect of reduction and alkylation on the accessibility of the V14 epitope and epitope mapping with a peptide array. The inability of V14 to detect PrP^{F198S} raises two possibilities: First, the residue Phe itself is a key element of the epitope and the F198S mutation completely blocks V14 binding. However, the residue Phe is out of the V14 epitope, as demonstrated by the X-ray crystallography study [18,17], which does not support this possibility. Second, although residue Phe itself is not part of the epitope, F198S mutation may affect the disulfide bond between residues 179 and 214, which blocks the accessibility of the V14 epitope. To rule out this possibility, we next used V14 to detect PrP treated with a reducing reagent tributylphosphine (TBP) and an alkylating reagent mechlorethamine (MCT) that break disulfide bond and block the free thiol group.

In addition to the V14 antibody, three other antibodies were used as controls: 3F4 directed against PrP105-112, 6H4 directed against PrP145-152 and anti-C against PrP220-231. All antibodies detected untreated recombinant human PrP23-231, while they also detected PrP in samples treated with TBP or MCT alone (Fig. 5). Treatment with TBP alone decreased the intensity of PrP probed with the four antibodies. However, V14 detected no PrP at all in samples treated with TBP and MCT together, while 3F4 and anti-C antibodies still detected PrP (Fig. 5). This result is similar to our previous observation with 6H4 [13,20].

We previously used peptide membrane array, a technique that has often been used to map antibody epitopes, to re-map epitopes of 1E4 and 3F4 antibodies [6,12]. However, here we were unable to find convincing epitopes for V14 and V61 antibodies using a 99 13-mer peptide membrane array that covers the entire human PrP sequence from residues 23 to 231 (data not shown). Our result is consistent with the observation reported by Moudjou et al. [16], suggesting that they have conformational epitopes even though they are able to detect the denatured PrP on Western blots.

Comparison of glycan modification between PrP^{T183A} and PrP^{F198S} by treatment with Endo H and PNGase F. We treated PrP^{Wt}, PrP^{T183A} and PrP^{F198S} with Endo H, or PNGase F that cleaves N-linked glycans. The Endo H treatment did not significantly change the gel profile and glycoform ratios of PrP^{Wt} (Fig. 6A). In contrast, it did significantly reduce the intensity of the monoglycosylated PrP^{T183A} and increase the intensity of its unglycosylated form (Fig. 6A). No relevant changes in the intensity of di-glycosylated PrP^{F198S} were observed, while the two monoglycosylated PrP^{F198S} species became undetectable after treatment with Endo H, suggesting that Endo H only removes glycans from monoglycosylated PrP at the two sites. On the other hand, a faint band migrating at ~28-29 kDa corresponding to the unglycosylated and deglycosylated PrP^{F198S} was visible in the treated sample, probably deriving from monoglycosylated PrP (Fig. 6A). After treatment with PNGase F, all three different PrP species were observed to have a band migrating at ~28-29 kDa corresponding to deglycosylated and unglycosylated PrP (Fig. 6A). However, only PrP^{Wt} and PrP^{F198S} exhibited a band migrating at ~20 kDa corresponding to endogenously N-terminally truncated fragment C2.

To confirm that Endo H only reduces monoglycosylated but not di-glycosylated PrP species, we proceeded to examine Endo H or PNGase F treated PrP^{F198S} with two more antibodies including anti-C and anti-N (Fig. 6B). Reaffirming evidence from the 3F4 antibody, both anti-C and anti-N antibodies also revealed no decreases in the intensity of the di-glycosylated PrP but dramatic decreases in the intensity of the monoglycosylated PrP species. PNGase F also removed all glycans from PrP^{F198S}. Using these two antibodies, we also examined PrP^{Sc} from sCJD and observed no changes in the intensity of both di- and mono-glycosylated PrP species after treatment with Endo H (Fig. 6C). Once again, PNGase F removed glycans from PrP^{Sc} as well.